Metallophysics and Advanced Technologies
Металофіз. новітні технол.
Metallofiz. Noveishie Tekhnol.
2026, vol. 48, No. 3, pp. 293–305
https://doi.org/10.15407/mfint.48.03.0293
Reprints available directly from the publisher

PACS numbers: 61.05.cp, 74.25.Fy, 74.25.Ha, 74.62.Bf, 74.62.Dh, 74.72.-h

Preparation of the $Bi_{2-x}Ag_xBa_{2-y}Sr_yCa_2CO_2Cu_3O_{10+\delta}$ High-Temperature Superconductor and Investigating the Effects of Single and Double Partial Substitution of Ag in Bi and Sr in Ba on Structural and Electrical Properties

M. A. Hamood, M. M. Al-Slivani, and N. A. Ismael

Department of Physics, College of Sciences, University of Mosul,
Al Majmoaa Str.,
41002 Mosul, Iraq

This study investigates the preparation of superconductor samples of $Bi_{2-x}Ag_xBa_{2-y}Sr_yCa_2CO_2Cu_3O_{10+\delta}$ using the solid-state reaction method with partial substitution of silver in both Bi and Ba at ratios of $x = 0$, 0.15, 0.25 and $y = 0$, 0.15, 0.25. X-ray diffraction is used to analyse the crystal structure, revealing a tetragonal structure with an increase in the *c*-axis length at an Ag substitution ratio of $x = 0.15$. Electrical-resistivity and critical-temperature (T_c) measurements are conducted using four-probe methods, showing an increase in T_c with Ag substitution up to $x = 0.15$, where T_c values reach 137.7 K and 162.5 K for the Ag-substituted samples. As observed, the oxygen content δ has a direct correlation with T_c, increasing as T_c improves. These results provide valuable insights into enhancing the properties of high-temperature superconductors through chemical substitutions and oxygen distribution, with promising implications for future applications in energy systems and magnetic-transportation technologies.

Key words: superconductor, solid-state reaction method, sintering and annealing process, structural and electrical properties.

Corresponding author: Mahmood Ahmed Hamood
E-mail: dr.mahmood@uomosul.edu.iq

Citation: M. A. Hamood, M. M. Al-Slivani, and N. A. Ismael, Preparation of the $Bi_{2-x}Ag_xBa_{2-y}Sr_yCa_2CO_2Cu_3O_{10+\delta}$ High-Temperature Superconductor and Investigating the Effects of Single and Double Partial Substitution of Ag in Bi and Sr in Ba on Structural and Electrical Properties, *Metallofiz. Noveishie Tekhnol.*, **48**, No. 3: 293–305 (2026). DOI: 10.15407/mfint.48.03.0293

Розглянуто одержання надпровідних $Bi_{2-x}Ag_xBa_{2-y}Sr_yCa_2CO_2Cu_3O_{10+\delta}$-зразків методом твердофазної реакції з частковим заміщенням Арґентумом як Bi, так і Ba у співвідношеннях $x = 0, 0{,}15, 0{,}25$ та $y = 0, 0{,}15, 0{,}25$. Для аналізи кристалічної структури було використано метод рентґенівської дифракції, за допомогою якого встановлено тетрагональну структуру зі збільшенням довжини осі c за заміщення Ag у співвідношенні $x = 0{,}15$. Вимірювання питомого електричного опору та критичної температури (T_c) проведено чотирозондовим методом і показано збільшення T_c із заміщенням Ag до $x = 0{,}15$, де значення T_c досягають 137,7 К та 162,5 К для зразків, заміщених Ag. Показано, що вміст Оксиґену δ має пряму кореляцію з T_c, збільшуючись з підвищенням T_c. Ці результати уможливлюють поліпшувати властивості високотемпературних надпровідників шляхом хемічних заміщень і розподілу Оксиґену, що може мати багатообіцяючі наслідки для їхнього майбутнього застосування в енергетичних системах і магнетотранспортних технологіях.

Ключові слова: надпровідник, метод твердотільних реакцій, процес спікання та відпалу, структурні й електричні властивості.

(Received 3 July, 2025; in final version, 15 October, 2025)

1. INTRODUCTION

Superconductivity is the phenomenon of electricity being transmitted smoothly through a material that exhibits no electrical resistance at extremely cold temperatures. This property is usually observed in metallic materials under deep freezing conditions [1]. Superconductivity involves two interrelated phenomena: the first is perfect conductivity and the second is absolute magnetism. Different materials exhibit superconductivity when they reach the T_c critical temperature value. The material switches from its initial state to its superconducting state at this specific temperature where each element has its unique critical temperature. Extensive ongoing research has described the enigmatic concept of superconductivity more clearly [2]. Modern superconductive materials find extensive usage in power transmission and magnetic technology sectors while boosting energy collection and magnetic transportation systems. These advanced materials display two main characteristics among others: zero electrical resistance and perfect conductivity with additional features of magnetism and the Meissner effect. The existing potential applications of superconductors drive scientists to conduct ongoing research within the field. The scientific examination of superconductors becomes essential because of their special characteristics while acknowledged applications across technological fields must be investigated. Superconductors continue evolving through two major categories, which distinguish type I and type II superconductors based on coherence length and critical temperature while their classification by critical temperature leads to identification of high and low temperature

superconductors including some cross-linked properties [3].

In 1911, the Dutch physicist Kamerlingh Onnes, during an investigation of the temperature dependence of electrical resistance in solid mercury (Hg) at very low temperatures using a liquid helium coolant found that it became totally resistant-free below 4.2 K or boiling point of liquid He known as superconductivity. It resulted in the discovery of a novel solid-state phenomenon: electric superconductivity [4]. More investigation into this wonderful phenomenon continued, and in 1933, Meissner and Ochsenfeld found one of the most crucial peculiarities in superconducting materials that are so-called ideal property; it refers to the fact that no magnetic field will pass through a material having zero-specific-resistance [5]. In the superconducting system Ba–La–Cu–O, which Bednorz and Müller discovered in 1986, there is a new class of superconducting material that is mostly formed of copper oxide. This compound is superconducting up to a critical temperature of ($T_c = 93$ K) [6]. Drolet *et al.* and Schilling subsequently [7] achieved T_c 133 K in Hg–Ba–Ca–CuO, then, they reported two new phases named Hg-1212 and Hg-1223 for related mercury-based series having composition of the form $n1n23$ so that there is no agreement on formula or structure. The $n = 1$ one member of this series, Hg-1201 with a tetragonal crystal structure maximal critical temperature $T_c = 95$ K and lattice parameters $a = 3.876$ Å and $c = 9.515$ Å [8]. In 2010, researcher Twessan examined the effect of partial substitution of the element Tl on the physical properties of the superconducting compound ($Bi_2Sr_2Ca_2Cu_3O_{10+\delta}$) at high temperatures, reaching a critical temperature of 136 K with a substitution ratio $x = 0.2$ by partial substitution of Tl with Bi, with the application of a hydrostatic pressure of 8 tons/cm^2 and an annealing temperature of 1123 K [9]. In 2010, researcher Razzaq and his time prepared samples of the high-temperature superconducting system $Bi_2Ba_2Ca_2Cu_3O_{10}$ using the solid-state reaction technique at different sintering temperatures including 810, 830, 850, 870, and 890°C. X-ray diffraction technique was used to analyse the crystal structure of the sample, and the results showed that the sample prepared at 850°C showed a tetragonal phase with fixed crystal lattice dimensions of $a = b = 5.42$ Å and $c = 34.13$ Å. Electrical resistivity measurements were performed on the samples, and the measurements revealed that the sample prepared at 850°C achieved a critical temperature T_c of 120 K, but it decreased to 87 K when prepared at 870°C. The sample prepared at 890°C showed semiconductor behaviour with activation energies of 8.593 and 3.456 meV. Research done on the sample from 850°C annealing demonstrated that the optimum critical temperature T_c reached 132 K after subjects it to 400°C annealing sessions. Research showed that critical temperature measurements rose to 140 K throughout the annealing period from 24 to 72 hours while oxygen content and Cu–O layer proliferation inside the cell were identified as factors responsible

for this change [10]. The research investigates how partial substitution of silver affects the high-temperature superconducting compound $Bi_{2-(0.15,\ 0.25)}Ag_{(0.15,\ 0.25)}Ba_{2-(0.15,\ 0.25)}Sr_{(0.15,\ 0.25)}Ca_2CO_2Cu_3O_{10+\delta}$. The research examines the structural and electrical aspect modifications, which result from silver substitution in the compound. The research utilizes solid-state reactions together with high-pressure techniques to evaluate how silver substitution changes crystal structure definitions as well as electrical resistivity and critical temperature measurements. The research shows that replacing some silver atoms results in structural and oxygen content changes, which enhances the electrical behaviour of the compound. Research findings help advance knowledge about how selective chemical changes can improve high-temperature superconductors and enable their use in energy transportation systems and magnetic technologies.

2. EXPERIMENTAL/THEORETICAL DETAILS

2.1. Materials

The Indian origin chemicals $AgNO_3$, $CaCO_3$, $Bi(NO_3)_2{\cdot}5H_2O$, CuO, $BaCO_3$ and $Sr(NO_3)_2$ as well as additional chemicals underwent a grinding procedure before reaching 99% purity levels. The procedure incorporated the usage of isopropanol C_3H_8O. An oxygenated atmosphere inside the convection furnace was achieved using oxygen gas (O_2) during annealing.

2.2. Devises and Tools

A precise measurement of powder weights required the usage of a Japanese M314Ai balance with ($\pm$ 0.0001) accuracy. A ceramic vessel produced in China served as the test container because it reaches temperatures up to 1200°C. A small mortar made of Japanese gate mortar was used to grind and mix the powders. The annealing and melting process was carried out using a British electric furnace (ELITE) located at the University of Mosul, College of Science, Department of Physics. A hydraulic press was also used to press the samples, which is available at the college of science, department of chemistry at the University of Mosul. The mould used to press the samples was locally made. To regulate the flow of oxygen gas to the electric furnace at a rate of 2 l/hour, a Japanese oxygen regulator was used.

2.3. Methods

The samples $Bi_{2-(0.15,\ 0.25)}Ag_{(0.15,\ 0.25)}Ba_{2-(0.15,\ 0.25)}Sr_{(0.15,\ 0.25)}Ca_2CO_2Cu_3O_{10+\delta}$

were generated at the ratios $x = 0$, 0.15, 0.25 and $y = 0$, 0.15, 0.25 using the solid-state reaction method. Equivalent amounts of powders were weighed using a high-precision sensitive balance, then combined and ground using an agate mortar, adding sufficient amount of isopropanol to ensure the formation of a homogeneous mixture. The grinding process continued for approximately 30 min. Then, the mixture was dried at temperatures between 40 and 50°C for approximately 30 min to remove excess isopropanol solution. The dried mixture was compressed using a hydraulic press to form 1.2 cm diameter discs under a pressure of 7.5 tons/cm^2. Then, the tablets were heated in a preheated oven to 800°C for 24 hours, at a heating rate of 120°/hour, and then cooled to room temperature at a rate of 30°C/hour. The annealing process was carried out in air.

In the second step, the compressed granules were ground and recompressed in the same way, and then placed in the oven. The temperature was gradually raised from room temperature to 600°C at a heating rate of 120°C/hour, and the granules remained at this temperature for about 10 hours. Then, the temperature was raised to 750°C at a heating rate of 120°C/hour, and the samples remained at this temperature for about 20 hours. Then, the samples were gradually cooled to 600°C at a rate of 30°C/hour, and remained at this temperature for about 10 hours. Finally, the samples were cooled to room temperature at a rate of 30°C/hour. Annealing was carried out using an oxygen-saturated atmosphere at a flow rate of 2 l/hour.

X-ray diffraction XRD: the structure and crystal structure have been verified by PANalytical Aeris machine that has following characteristics shown in Table 1.

The following relation was used to compute the relative volume fraction of any phase [11, 14]:

$$V_{\text{ph}} = \frac{I_0}{I_0 + I_1 + I_2 + \ldots + I_n} \times 100\,, \qquad (1)$$

TABLE 1. Characteristics of the x-ray diffraction machine that used.

Source	Cu target
Current	40 mA
Voltage	40 kV
Scan range	10–90°
Scan mode	Bragg–Brentano (θ–2θ) reflection geometry
Wave length	1.15406
Pre-set time	1 to 100 seconds
Scan speed	Up to 10°/min

where I_1, I_2, ..., I_n are the peaks intensity of all XRD, and I_0 is the XRD peak intensity of the phase that was determined.

Four-probe DC methods: The critical temperature T_c and resistivity ρ were measured using four probe DC methods. This relation can be used to determine the critical temperature [11, 15]:

$$\rho = \frac{RA}{L}, \tag{2}$$

where L is the length of the specimens, A is the area of the specimens, and R is their electrical resistance. The oxygen content was determined using the iodometric titration method.

Titration chemical method to determine the percentage of oxygen δ: 100 mg of the sample is taken and ground well using an agate mortar to obtain the repair powder.

Isopropanol is added to it to dry it completely; then, the sample is placed in a glass beaker clean of any chemical added to the powder 10 ml of iodide and became KI and 5 ml of hydrochloric acid HCl, which is a device for mixing the components using a magnet bar inside the magnetic stirrer and for the input port. After that, oxygen thiosulfate is prepared and the ratio is of 0.015, when adding KI and HCl, and the integration of the solution colours. Then, the elements of the element thiosulfate were added until it became dark brown, and at this stage, the addition is eliminated. Completely, the dissolved construction was added, which changed the colour of the solution from change to the new blue, indicating the freedom of iodine. Then continue to add descriptive thiosulfate until Namibia, in addition to the complementary colours in addition to the colour. At this moment, the amount of oxygen thiosulfate is added, and the solution used in the regeneration process is recorded. The oxygen percentage δ was calculated using the following equation [12]:

$$\delta = \frac{\frac{M_A}{M_B} - \frac{3m_a}{C}}{\frac{2m_b}{CV} - \frac{M_o}{M_A}}, \tag{3}$$

since δ represents the percentage of oxygen in the sample, M_A represents the molecular weight of the sample, M_B represents the molecular weight of sodium thiosulfate $Na_2S_2O_3{\cdot}5H_2O$ = 248.18 mg, M_o represents the atomic weight of auxin (15.999), m_a represents the weight of the sample, m_b represents the mass of sodium thiosulfate used, which depends on the concentration of sodium thiosulfate, CV is the volume of the solution used in the titration, which we get from the relationship: $M_B = CV$, V represents the volume of sodium thiosulfate solution used in the titration, C represents the concentration of sodium thiosul-

fate solution equal to 0.015 g/mol.

3. RESULTS AND DISCUSSION

3.1. Study of the Structural Properties

The structural properties of the compound were studied at an annealing temperature 750°C and a pressure of 7.5 tons/cm^2, using Bragg's law, the distances between parallel planes d_{hkl} and Miller coefficients hkl were calculated based on the reflection angles 2θ using the (X'Pert Highscore) program, the dimensions of the unit cell a, b, c were determined, which showed that the structure is of the tetragonal type. Table 2 shows the values of the axes a, b, c after the annealing process.

The x-ray diffraction (XRD) study showed regularity in the crystal structure and the appearance of clear peaks, as shown in Fig. 1, *a* for

TABLE 2. Results of the compositional examination of the compound $Bi_{2-(0.15,\ 0.25)}Ag_{(0.15,\ 0.25)}Ba_{2-(0.15,\ 0.25)}Sr_{(0.15,\ 0.25)}Ca_2CO_2Cu_3O_{10+\delta}$ at $x = 0,\ 0.15,\ 0.25$, $y = 0,\ 0.15,\ 0.25$.

Sample	a, Å	b, Å	c, Å	c/a	V, Å^3	V_{Ph}
$x = y = 0$	4.28	4.28	24.48	5.719	446.70	0.544
$x = 0.15, y = 0$	4.315	4.315	24.60	5.701	459.09	0.583
$x = 0.25, y = 0$	4.31	4.31	24.53	5.691	455.67	0.548
$x = 0.25, y = 0.15$	4.32	4.32	24.57	5.69	458.53	0.571
$x = 0.25, y = 0.25$	4.30	4.30	24.55	5.71	453.93	0.550

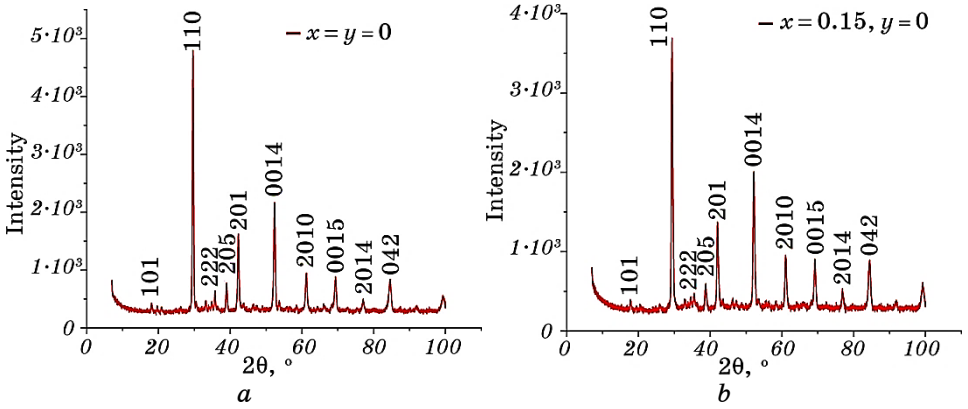

Fig. 1. X-ray diffraction of $Bi_{2-(0.15,\ 0.25)}Ag_{(0.15,\ 0.25)}Ba_{2-(0.15,\ 0.25)}Sr_{(0.15,\ 0.25)}Ca_2CO_2Cu_3O_{10+\delta}$ compound at $x = 0,\ 0.15,\ 0.25$, $y = 0,\ 0.15,\ 0.25$.

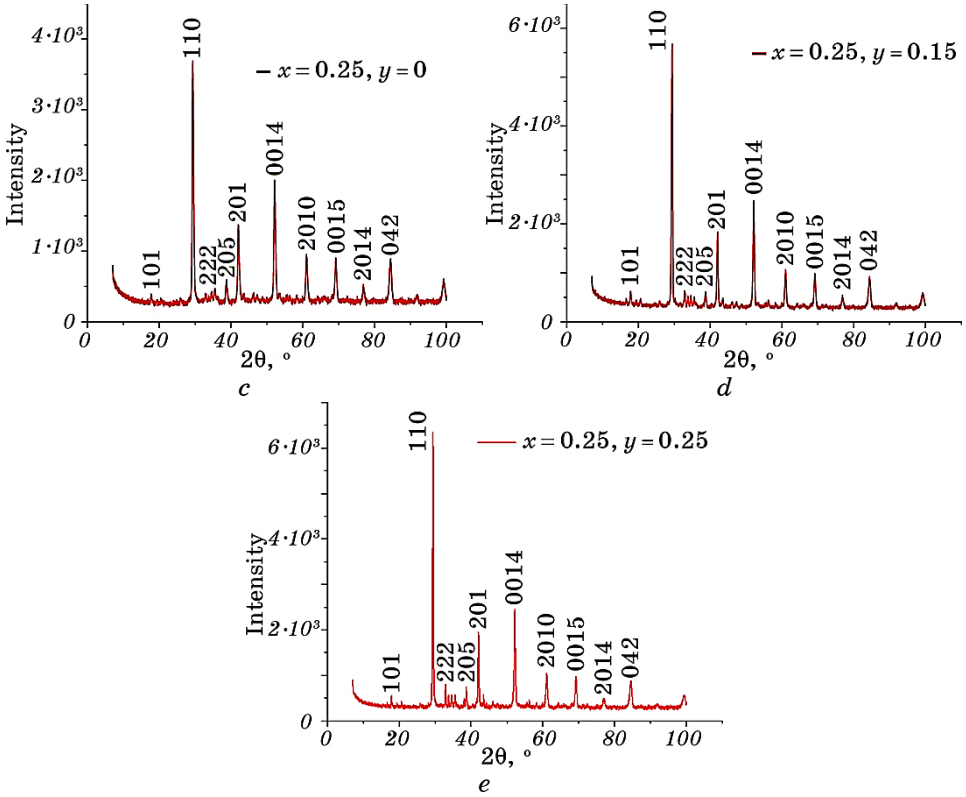

Continuation of Fig. 1.

the first standard sample $x = y = 0$ and the dimensions of the cell were $a = b = 4.28$ Å and $c = 24.48$ Å.

At a compensation ratio of $x = 0.15$, $y = 0$ the XRD results showed that the crystal structure remained tetragonal with clear peaks, and the lattice dimensions were $a = b = 4.315$ Å and $c = 24.60$ Å, as shown in Fig. 1, *b*. With increasing the compensation ratio to $x = 0.25$, $y = 0$, a decreased in the intensity and regularity of the peaks was observed, while the tetragonal crystal structure remained, and an increase in the length of the *c* axis. The lattice dimensions were $a = b = 4.31$ Å and $c = 24.53$ Å, confirming the improvement of the crystal structure of the compound as shown in Fig. 1, *c*, with an increase in the grain size. At the compensation ratio $x = 0.25$, $y = 0.15$ the peaks showed greater clarity compared to the previous compensations with an increase in the length of the *c* axis, indicating an increase in the crystalline regularity, where the lattice dimensions were $a = b = 4.32$ Å and $c = 24.57$ Å, as shown in Fig. 1, *d*. As for the compensation ratio $x = 0.25$, $y = 0.25$, a decrease in the intensity of the peaks was observed, as shown in Fig. 1,

e, indicating a decrease in the previous crystalline regularity as a result of increasing the compensation ratio, where the lattice dimensions were $a = b = 4.30$ Å and $c = 24.55$ Å with a clear decrease in the length of the *c* axis. Through this study, we conclude that the best partial compensation ratio for the Ag element in Bi in the 2223 system is when $x = 0.15$. The importance of the tetragonal structure lies in its crystal stability, which allows for a balanced distribution of oxygen within the lattice, enhancing the electronic structure and contributing to the improvement of the critical temperature T_c. Furthermore, changes in the crystal dimensions, especially the *c* axis, have a direct impact on the distribution of gap carriers in the material, contributing to the material's enhanced superconductivity. This relationship between crystal structure and electrical conductivity highlights the importance of choosing the optimal silver substitution ratio to achieve the best conductive performance, as suggested by studies on high-temperature superconductors such as those by Combescot (2022) [1] and Al-Slivani *et al.* (2025) [14] who demonstrated the role of lattice optimization in enhancing superconducting properties.

3.2. Study of the Electrical Properties

The electrical properties of $Bi_{2-(0.15,\ 0.25)}Ag_{(0.15,\ 0.25)}Ba_{2-(0.15,\ 0.25)}Sr_{(0.15,\ 0.25)}Ca_2CO_2Cu_3O_{10+\delta}$ compound were studied when Ag was partially replaced in Bi at different ratios of at $x = 0, 0.15, 0.25$, $y = 0, 0.15, 0.25$.

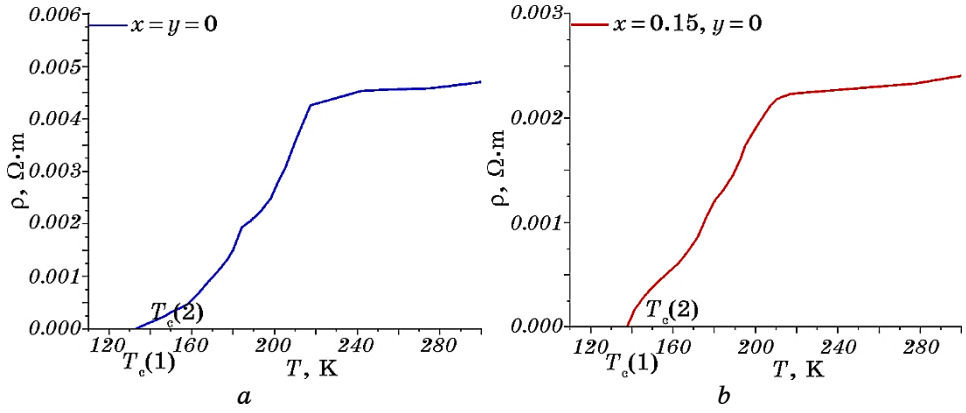

Fig. 2. Shows the relationship between the resistivity and the critical temperature of $Bi_{2-(0.15,\ 0.25)}Ag_{(0.15,\ 0.25)}Ba_{2-(0.15,\ 0.25)}Sr_{(0.15,\ 0.25)}Ca_2CO_2Cu_3O_{10+\delta}$ compound at a compensation ratio: $x = y = 0$ (*a*), $x = 0.15$, $y = 0$ (*b*), $x = 0.25$, $y = 0$ (*c*), $x = 0.25$, $y = 0.15$) (*d*), and $x = 0.25$, $y = 0.25$ (*e*). The drawing illustrates how resistivity varies with falling temperature until reaching critical temperature.

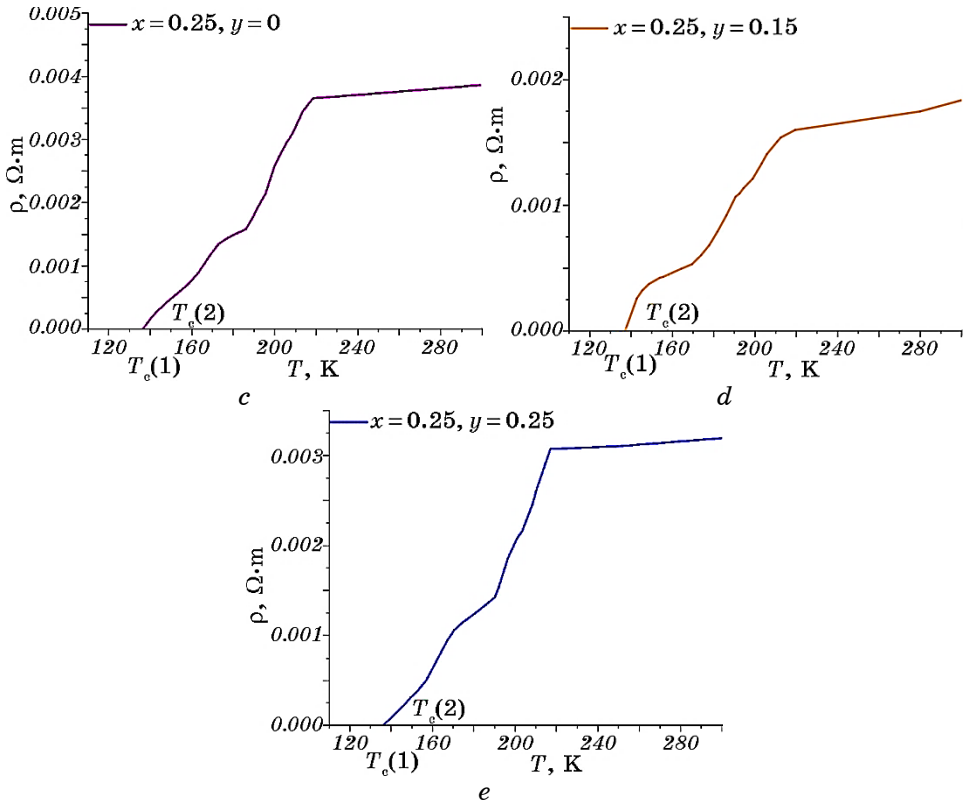

Continuation of Fig. 2.

The results showed that at the compensation ratio $x = y = 0$, the critical temperature was $T_c(1) = 133$ K, $T_c(2) = 153.5$ K, as shown in Fig. 2, *a*, which is the pure standard sample. With increasing the compensation ratio to $x = 0.15$, $y = 0$, an increase in the critical temperature was observed to become $T_c(1) = 137.7$ K, $T_c(2) = 162.5$ K, as shown in Fig. 2, *b*. As for the compensation ratio $x = 0.25$, $y = 0$, an increase in the critical temperature was observed to $T_c(1) = 136.4$ K, $T_c(2) = 158.5$ K, as shown in Fig. 2, *c*. At a compensation ratio of $x = 0.25$, $y = 0.15$, the critical temperature increased to $T_c(1) = 137.1$ K, $T_c(2) = 159.1$ K, which can be explained by the fact that the compound became more regular in the crystal structure, with the increase in the oxygen ratio, which makes this ratio the best among the studied ratios, as shown in Fig. 2, *d*. As for compensation of $x = 0.25$, $y = 0.25$, a decrease in the critical temperature was observed to $T_c(1) = 135.7$ K, $T_c(2) = 156.9$ K, as shown in Fig. 2, *e*.

These results emphasize the critical role of oxygen content in determining the superconducting properties of the samples. Higher oxy-

TABLE 3. Shows the relationship between the compensation ratio x, the critical temperature T_c, and the percentage of oxygen δ in the compound $Bi_{2-(0.15,\ 0.25)}Ag_{(0.15,\ 0.25)}Ba_{2-(0.15,\ 0.25)}Sr_{(0.15,\ 0.25)}Ca_2CO_2Cu_3O_{10+\delta}$.

Sample	$T_c(1)$, K	$T_c(2)$, K	ΔT_c, K	T_c(mid), K	δ
$x = y = 0$	133	153.5	20.5	143.25	0.332
$x = 0.15$, $y = 0$	137.7	162.5	24.8	150.1	0.415
$x = 0.25$, $y = 0$	136.4	158.5	21.6	147.2	0.387
$x = 0.25$, $y = 0.15$	137.1	159.1	22	148.1	0.397
$x = 0.25$, $y = 0.25$	135.7	156.9	21.2	146.3	0.371

gen levels contribute to better phase homogeneity and improved critical temperatures, underscoring the interplay between oxygen concentration, composition, and multiphase behaviour in these compounds [13–16]. Table 3 shows the values of the critical temperature and the oxygen ratio δ for each compensation ratio.

Oxygen content is a crucial element in determining the superconducting properties of compounds. Oxygen content directly affects the distribution of hole carriers in the crystal lattice, contributing to the improvement of the material's electrical conductivity. When there is an optimal balance of oxygen within the crystal structure, the concentration of hole carriers is enhanced, enhancing the material's superconductivity [17]. Increasing the oxygen concentration in a material improves structural homogeneity, which contributes to reducing crystal defects and increasing lattice stability. This improvement in homogeneity enhances crystal regularity and reduces distortions that could impede the movement of hole carriers. This, in turn, leads to an increase in the critical temperature T_c, as improvements in oxygen distribution contribute to enhanced conductive performance of the material [18]. In addition, substituting or changing oxygen in the crystal structure leads to changes in the electronic energy states, which directly influences conductive properties. Therefore, it is necessary to explore the precise relationship between oxygen content and superconducting properties more deeply, to understand its impact on gap carrier concentration and critical temperature T_c, and to improve the overall performance of superconducting materials [19].

4. CONCLUSION

In this study, we have examined superconductor compounds $Bi_{2-(0.15,\ 0.25)}Ag_{(0.15,\ 0.25)}Ba_{2-(0.15,\ 0.25)}Sr_{(0.15,\ 0.25)}Ca_2CO_2Cu_3O_{10+\delta}$ synthesized by solid state reaction technique for $x = 0$, 0.15, 0.25 and $y = 0$, 0.15, 0.25. The XRD pattern analysis revealed a tetragonal structure with a

high ratio of the Bi-2223 superconductor phase. Additionally, the Ag-doped sample at $x = 0.15$, $y = 0$ showed a highest increased in the axial length c.

In the $Bi_{2-(0.15,\ 0.25)}Ag_{(0.15,\ 0.25)}Ba_{2-(0.15,\ 0.25)}Sr_{(0.15,\ 0.25)}Ca_2CO_2Cu_3O_{10+\delta}$ complex, the optimal substitution ratio for Ag is found at $x = 0.15$, $y = 0$, where a significant proportion of phase Bi-2223 is seen. This is the optimal value for x. Undoped Bi-2223 had critical temperature $T_c(1) = 133$ K, $T_c(2) = 153.5$ K.

The $Bi_{2-(0.15,\ 0.25)}Ag_{(0.15,\ 0.25)}Ba_{2-(0.15,\ 0.25)}Sr_{(0.15,\ 0.25)}Ca_2CO_2Cu_3O_{10+\delta}$ compounds have shown a maximum value of critical temperature $T_c(1) = 137.7$ K, $T_c(2) = 162.5$ K at $x = 0.15$, $y = 0$, when Ag is substituted for it. In addition, oxygen content δ have been found increases with increasing critical temperature T_c since the substitution produced of local pressure, hole carrier concentration, variation electronic state and its distribution.

AUTHORS' CONTRIBUTIONS

M. A. Hamood conceptualized and designed the project, supervised the research findings, and reviewed the final manuscript. M. M. Al-Slivani performed the preparation of the superconductor samples using the solid-state reaction method, conducted the x-ray diffraction tests, and performed the electrical resistivity measurements. N. A. Ismael carried out the iodometric titration method to determine the oxygen percentage, calculated the relative volume fractions and unit cell dimensions using the X'Pert Highscore program, and drafted the manuscript. All authors discussed the structural and electrical results, verified the analytical approaches, and approved the final version of the manuscript.

REFERENCES

1. R. Combescot, *Superconductivity* (Cambridge: Cambridge University Press: 2022).
2. M. A. Hamood, *Rafidain J. Sci.*, **27**, No. 1: 307 (2018).
3. M. Rizwan, A. Ayub, S. Fatima, I. Ilyas, A. Usman, and A. Shoukat, *Mater. Research Foundations*, **132**: 49 (2022).
4. H. K. Onnes, *Comm. Phys. Lab. Univ. Leiden*, **12**: 120 (1911).
5. W. Meissner and R. Ochsenfeld, *Naturwissenschaften*, **21**: 787 (1933).
6. J. G. Bednorz and K. A. Müller, *Zeitschrift für Physik B*, **64**: 189 (1986).
7. A. Schilling, M. Cantoni, and J. D. Gao, *Nature*, **363**: 56 (1993).
8. M. Paranthaman, J. R. Thompson, and Y. R. Sun, *Physica C*, **213**, Iss. 3–4: 271 (1993).
9. T. M. Twessan, *Thesis of Disser. for Master* (Tikrit: University of Tikrit: 2010).
10. K. H. Razeg, K. D. Alazawi, and M. A. Hmood, *J. Edu. Sci.*, **24**, No. 4: 114 (2010).
11. M. M. Al-Slivani, M. A. Hammod, and M. A. Abed, *Ochrona przed Korozją*, **1**,

No. 3: 15 (2025).
12. C. Baird and M. Cann, *Environmental Chemistry* (W. H. Freeman and Company: 2009).
13. K. A. Jasim and L. A. Mohammed, *J. Phys.: Conf. Series*, **1003**: 012071 (2018).
14. M. M. Al-Slivani, M. A. Hammod, and M. A. Abed, *Functional Mater.*, **32**: 42 (2025).
15. K. A. Jasim, C. A. Z. Saleh, and A. H. A. Jassim, *Korean J. Mater. Research*, **34**, Iss. 1: 21 (2024).
16. A. H. A. Jassim, C. A. Z. Saleh, and K. A. Jasim, *AIP Conf. Proc.*, **2769**, Iss. 1: 020022 (2023).
17. S. Wakimoto, R. J. Birgeneau, Y. S. Lee, and G. Shirane, *arXiv:cond-mat/0011392* (2001).
18. Z. Hu, M. S. Golden, S. G. Ebbinghaus, M. Knupfer, J. Fink, and F. M. F. de Groot, *Chem. Phys.*, **282**: 451 (2002).
19. N. Kowalski, S. S. Dash, D. Sénéchal, and A.-M. S. Tremblay, *arXiv:2104.07087* (2021).